

# Sharp luminescent lines from single three-dimensionally confined GaAs/AlAs structures grown on a patterned GaAs substrate

Jun-ichi Kasai, Sige-hisa Tanaka, and Katsuhiko Higuchi

*Central Research Laboratory, Hitachi, Ltd., 1-280 Higashi-koigakubo, Kokubunji, Tokyo 185-8601, Japan*

Yoshifumi Katayama\*

*Optoelectronics Technology Research Laboratory, 5-5 Tohkodai, Tsukuba, Ibaraki 300-2635, Japan*

(Received 2 March 1998; revised manuscript received 25 September 1998)

We report extremely sharp lines of photoluminescence (PL) and photoluminescence excitation (PLE) spectra from single three-dimensionally confined GaAs/AlAs structures grown on square mesas patterned onto a GaAs substrate. The single structures, which had a 10-nm vertical thickness and a 0.2- $\mu\text{m}$  lateral width, were measured at 8 K by microphotoluminescence. At high-excitation power, the PL and PLE spectra of the single structures exhibited broad exciton peaks several meV wide. However, when the excitation power was lowered, each heavy-hole exciton peak in the PL and PLE spectra became a series of sharp lines whose widths were respectively, about 0.5 and 0.3 meV. The sharp lines of the PL spectra were probably due to the radiative recombination of excitons localized into lateral potential islands in the single structure. In the PL spectrum at a lower excitation power, a sharp line split into extremely sharp lines ( $\cong 0.04$  meV). This fine splitting possibly represents a difference in the confinement energy of excitons localized in potential islands that have almost the same local thickness but differ in size and microstructure. From our analysis of the PLE spectra and the resonant PL spectra, we conclude that a sharp line in a PLE spectrum is not directly related to any particular sharp line of a PL spectrum. The sharp lines of the PLE spectra can be interpreted in terms of exciton absorption whose energy is determined by the locally averaged thickness of the single structure.

[S0163-1829(99)00443-9]

## I. INTRODUCTION

Modulation of band-gap energy in three dimensions allows spatial confinement of charge carriers to within small volumes. For extremely small confining potential wells, three-dimensional quantum effects become significant. The investigation of these extremely small confined structures, i.e., quantum dots, has received considerable attention due to their atomlike energy levels with a discrete density of states that can be used for novel device applications.<sup>1-3</sup>

Various attempts have been made to fabricate quantum dots. One fabrication technique is based on spontaneous island formation during epitaxial growth on lattice-mismatched substrates.<sup>4,5</sup> All interfaces of three-dimensionally (3D) confining potential wells are formed *in situ* and can be made free of contamination. Optical measurements of the 3D-confined structures fabricated by this self-assembling method have revealed the emission of extremely sharp luminescent lines.<sup>6-8</sup> These sharp luminescent lines are believed to be evidence of a discrete density of states and, consequently, of the successful fabrication of quantum dots. However, it is difficult to control the density and position of the structures by the self-assembling method. This difficulty is especially undesirable for device applications.

Another approach to fabricating quantum dots is based upon epitaxial growth on patterned substrates.<sup>9</sup> This method takes advantage of the difference in growth rates on neighboring facets. As in the self-assembling method, all interfaces of 3D-confined structures are formed during the growth process. The density and position of the structures are controlled by pre patterning of substrates. There have been sev-

eral reports on 3D-confined structures fabricated by this growth method.<sup>10-16</sup> Madhukar, Rajkumar, and Chen obtained evidence of 3D-confined structures with lateral sizes down to about 50 nm by observing cross sections of grown pyramidal structures with a transmission electron microscope.<sup>10,13</sup> The cathodoluminescence (CL) spectra of the 3D-confined structures indicated their high-optical quality.<sup>11,13,16</sup> However, although the sizes of the 3D-confined structures were within the regime of three-dimensional quantum confinement, their CL spectra exhibited broad peaks (about 10 meV wide) and, consequently, did not exhibit sharp luminescent lines.

One possible origin of this broadening was thought to be the stacked multiple layers of the 3D-confined structures, which had slightly different respective thicknesses. To eliminate this possible cause of broadening, we fabricated a single layer of 3D-confined structures instead of multiple layers by growing a single quantum-well (QW) heterostructure on a patterned substrate.<sup>17</sup> Although the lateral sizes of the obtained structures were of the submicrometer order, i.e., not within the quantum-confinement regime, extremely sharp luminescent lines were observed when measuring the low-temperature microphotoluminescence of the single structures. In this paper, we examine these extremely sharp lines of photoluminescence (PL) and photoluminescence excitation (PLE) spectra from the single 3D-confined structures, and discuss the origins of the sharp luminescent lines in terms of heterointerface fluctuations.

## II. FABRICATION OF CONFINED STRUCTURES

The 3D-confined structures on patterned substrates are formed by growth on mesa structures whose top facet is sur-

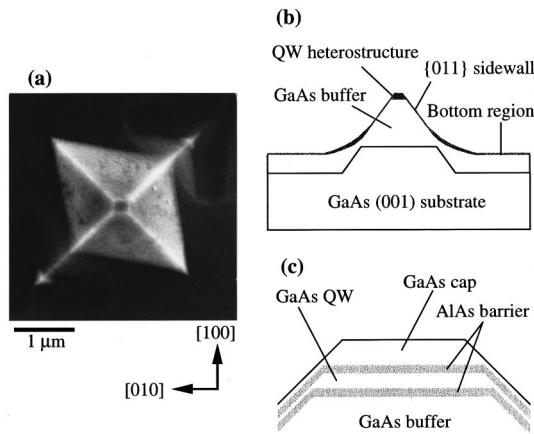


FIG. 1. (a) SEM top-view image of a truncated pyramid structure after growth on a 3.0- $\mu\text{m}$ -side mesa. The mesa-top shape of the pyramid is a square with 0.2- $\mu\text{m}$  sides. (b) Schematic cross section of the truncated pyramidal structure. (c) Enlarged view of the mesa-top region of (b).

rounded by crystallographically equivalent side facets. In our study, square mesa structures were patterned with sides oriented along the  $\langle 100 \rangle$  directions on a GaAs (001) substrate. The equivalent side facets were the  $\{011\}$  planes. The patterning was done by electron-beam lithography followed by wet chemical etching at 24 °C. The negative-type resist was SAL601 (Shipley) and the etchant was  $\text{H}_3\text{PO}_4:\text{H}_2\text{O}_2:\text{H}_2\text{O}$  (1:2:40). The square mesas had lateral widths of 2.8–4.2  $\mu\text{m}$  with an interval of 0.2  $\mu\text{m}$  after etching. The size variation allowed us to fabricate single 3D-confined structures of various lateral widths on spatially isolated mesa structures in the same growth run.

Epitaxial growth was done in a conventional molecular-beam-epitaxy system. The growth structure consisted of a GaAs buffer layer (700 nm), AlAs/GaAs/AlAs QW layers (10/5/10 nm), and a GaAs capping layer (10 nm). The layer thickness was determined in a flat region of the substrate, and the growth rates of GaAs and AlAs were both 0.5  $\mu\text{m}/\text{h}$ . The growth temperature, which was monitored by a thermocouple placed on the rear of the substrate, was 660 °C. The As beam equivalent pressure was  $7 \times 10^{-6}$  torr, and the substrate rotation during growth was 20 rpm.

During growth on patterned substrates, group-III atoms arriving at the sidewall facets migrate towards the adjacent facet of the mesa-top plane. This adatom migration results in a lower growth rate on the sidewalls than on the mesa top and in shrinkage of the mesa-top area, leading to mesa pinch off. The structure grown on the smallest square mesa in our experiment was a pinched-off pyramid limited by the  $\{011\}$  sidewall facets. Since the growth of QW heterostructures on patterned substrates causes lateral variations in layer thickness, 3D-confined structures are formed by growing QW heterostructures on pyramidal structures before the pinch off. Figure 1(a) is a scanning electron microscope (SEM) top-view image of a truncated pyramid structure grown on a 3.0- $\mu\text{m}$ -side square mesa. Figure 1(b) is a schematic cross-section of the truncated pyramidal structure. An enlarged view of the mesa-top region is shown in Fig. 1(c).

In the 3D-confined structure formed at the mesa top, the vertical confinement energy is due to quantum confinement introduced by the QW heterostructure. The lateral thickness

variations result in effective band-gap modulation, i.e., a lateral-position dependence of the vertical confinement energy. The thicker QW sections constitute lateral potential wells that can trap charge carriers, while the thinner QW sections function as effective lateral barriers that are analogous to the higher band-gap layers that serve as vertical barriers in conventional QW heterostructures.

As shown in the SEM image of Fig. 1(a), the mesa-top shape of the truncated pyramidal structures is a square. This shape reflects the lateral feature of the single 3D-confined structures embedded in the pyramidal structures. As mentioned above, the confining potential wells in the lateral directions were due to the lateral variations in the QW layer thicknesses of the mesa top and of the sidewalls. If the capping layer thickness is much less than the mesa-top width, the lateral width of the 3D-confined structures can be estimated from the mesa-top width after growth. The SEM observation therefore enables us to estimate the lateral width in the 3D-confined structures. The lateral width decreased from 1.6 to 0.2  $\mu\text{m}$  in proportion to a decrease in the pattern width.<sup>17</sup> In this paper, we report the results of detailed optical measurements of single 3D-confined structures that had the smallest lateral width of 0.2  $\mu\text{m}$ .

### III. OPTICAL PROPERTIES OF SINGLE CONFINED STRUCTURES

The optical measurements of the 3D-confined structures were taken by a low-temperature microphotoluminescence method based on confocal microscopy. This microscopy is a form of scanning optical microscopy using far-field optics.<sup>18</sup> High-spatial resolution is attained by scanning a focused spot of excitation light on an object in the confocal arrangement, where there is an aperture on the image focal plane that corresponds to the excitation spot. The optical setup used here was the same as in our previous reports.<sup>17,19</sup> In the present study, the aperture in the confocal arrangement was a 50  $\mu\text{m}$ -diameter pinhole, which gave a spatial resolution of less than 0.7  $\mu\text{m}$ . The excitation sources were an Ar-ion laser and a tunable Ti:sapphire laser. All measurements were done at a sample temperature of 8 K.

When we measured the PL spectra of a truncated pyramidal structure with low-spatial resolution attained by defocusing the laser beam and removing the pinhole aperture, the resultant spectra exhibited several luminescent peaks. These peaks spatially originated in various QW layers included in the pyramidal structure.<sup>17</sup> However, from the measurements where only the mesa-top region was illuminated with high spatial resolution, we observed a distinct luminescent peak due to emissions from the single 3D-confined structure embedded in the pyramid. The attribution of the peak to the 3D-confined structure was verified by PL images obtained by detecting luminescent light while scanning a focused spot of excitation light across the pyramidal structure. Thus, we were able to apply spectroscopy to single 3D-confined structures by positioning and holding the mesa-top region of one spatially isolated pyramidal structure at a time under the laser illumination.

Figure 2 shows the PL spectra of a single 3D-confined structure at various excitation powers. The excitation energy of 2.409 eV corresponds to the barrier excitation, where car-

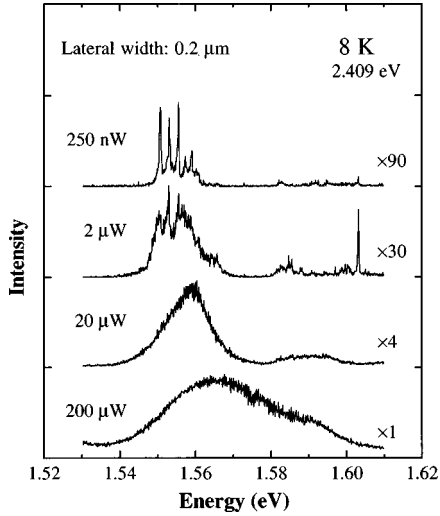


FIG. 2. PL spectra of a single 3D-confined structure at various excitation powers. The excitation energy was 2.409 eV, corresponding to the barrier excitation.

riers are generated both in the AlAs barrier layers and in the GaAs QW layer. The spectrum at an excitation power  $P_{\text{exc}}$  of 200  $\mu\text{W}$  exhibits a broad peak about 30 meV wide with a shoulder at the higher-energy side. At  $P_{\text{exc}}$  of 20  $\mu\text{W}$ , the main peak shifted to a lower energy and became sharper. Also, the shoulder became a distinct peak. PL image measurements revealed that the shoulder peak corresponds to emissions from a QW heterostructure around the base region of the pyramidal structure.<sup>17</sup> When the excitation power was further reduced to 250 nW, the main peak shifted to a still lower energy and became a series of sharp lines whose width was about 0.5 meV.

Since the lateral width of the 3D-confined structure was about 0.2  $\mu\text{m}$ , it can be regarded as a conventional QW heterostructure and, consequently, its vertical thickness can be estimated from the emission wavelength. The thickness estimated from the main peak at  $P_{\text{exc}}$  of 20  $\mu\text{W}$  was about 10 nm, which was much larger than the designed value. This large value indicates efficient adatom migration from the sidewalls to the mesa top in the pyramidal structure during crystal growth.

The sharpening and shift of the main peak was mainly explained by a reduction of the band-filling effect. We then estimated the density of electron-hole pairs generated by laser illumination in the single 3D-confined structure. In the case of well excitation, where carriers are generated only in the QW layer, the time-averaged pair number in the single structure  $N_{\text{pair}}$  was estimated as  $N_{\text{pair}} \cong \alpha \gamma \tau N_{\text{photo}}$ .<sup>20</sup> The number of photons  $N_{\text{photo}}$  that impinge on the sample per second follows directly from the measured excitation laser power  $P_{\text{exc}}$  via  $N_{\text{photo}} = P_{\text{exc}} / \hbar \omega$  ( $\hbar \omega$ : photon energy). The factor  $\gamma$  describes the ratio of the laser spot profile to the actual lateral size. Since a laser beam of 1.58 eV (a typical value in the well-excitation case) was focused to a 1.4- $\mu\text{m}$  spot,  $\gamma$  was about 0.053. An absorption probability of  $\alpha = 1 \times 10^{-2}$  was used as a typical value for the GaAs QW. The carrier lifetime  $\tau$  was assumed to be 300 ps.<sup>21</sup> Thus, for the highest excitation power of 200  $\mu\text{W}$  in the well-excitation case, the estimated pair number  $N_{\text{pair}}$  was 130.

For barrier excitation, which is the case in Fig. 2, the pair

number was also estimated as  $N_{\text{pair}} \cong \alpha \gamma \tau N_{\text{photo}}$ , but in this case the factor  $\gamma$  describes the ratio of carriers trapped in the QW layer to the number of photogenerated carriers. Unfortunately, the trapping efficiency of the carriers depends on the shape of the confining potential wells and changes from sample to sample. However, if we assume that the PL intensity is proportional to the pair number, measurements of the PL spectra caused by well and barrier excitation at the same power enable estimation of the pair number in the barrier-excitation case. Since the PL spectra in the barrier-excitation case were approximately nine times more intense than those in the well-excitation case, the pair number was estimated to be  $N_{\text{pair}} = (130 \times 9) \cong 1200$  at the highest power of 200  $\mu\text{W}$  in the barrier-excitation case. Consequently, the pair density in the single 3D-confined structure having a 10-nm vertical thickness was  $3 \times 10^{12} \text{ cm}^{-2}$ . This density is high enough to bring about the band-filling effect.

The change in the main peak may also involve the possible effects of plasma formation. There is a transition from an insulating exciton state to a metallic electron-hole plasma state in QW's.<sup>22</sup> The transition is generally expected to occur under the condition  $(n_{\text{ex}})^{1/2} \cdot (a_B) \geq 1$ , where  $n_{\text{ex}}$  is the exciton sheet density and  $a_B$  is the excitonic Bohr radius in QW's. This condition means that the average distance between excitons is comparable to or smaller than the excitonic Bohr radius. If  $a_B$  is approximated by the exciton radius in bulk GaAs ( $\cong 11$  nm),  $(n_{\text{ex}})^{1/2} \cdot (a_B)$  amounts to 1.9 in the highest-excitation case. Thus, the PL spectrum at the highest excitation power is expected to contain many-body effects in the electron-hole plasmas, for example, the band-gap renormalization. In fact, broadening on the low-energy side of the main peak was clearly observed (Fig. 2), indicating large band-gap renormalization.

In the PL spectrum at the lowest excitation power (Fig. 2), three intense and three weak lines were clearly resolved. We will focus first on the intense sharp lines, and will later discuss the weak sharp lines in connection with the PLE spectra. The energy spacing of the intense sharp lines was about 2.5 meV, which was nearly equal to the calculated energy produced by monolayer fluctuation in the QW thickness. The sharp lines can thus be interpreted as emissions from the radiative recombination of excitons localized at potential islands created by steps of monolayer height.<sup>23</sup> Figure 3(a) is a schematic of a heterointerface configuration that contains monolayer fluctuations. The rough interface configuration results in lateral variation of exciton confinement energy in the QW as shown in Fig. 3(b). At low temperatures, correlated electron-hole pairs or excitons become localized into island-like regions of the QW layer that are a few monolayers wider than the surrounding region and, consequently, have a smaller confinement energy. As shown in the PL spectrum of Fig. 3(b), the radiative recombination of the localized excitons leads to several sharp luminescent lines whose energy spacing corresponds to a thickness difference of one monolayer.

Figure 4 shows the PLE spectra of the single 3D-confined structure at  $P_{\text{exc}} = 20$  and 2  $\mu\text{W}$ , including its PL spectrum<sup>24</sup> where the well-excitation energy and power were 1.5818 eV and 2  $\mu\text{W}$ , respectively. The energy used to detect the PLE spectra was equal to the energy at which one of the sharp PL lines occurred in the bottom PL spectrum. At  $P_{\text{exc}}$  of 20  $\mu\text{W}$

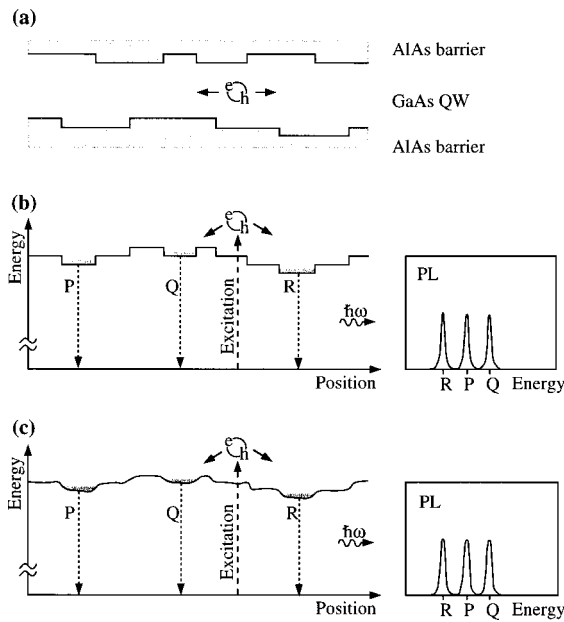


FIG. 3. (a) Schematic illustration of an interface configuration containing steps of monolayer height. (b) Exciton confinement energy corresponding to the interface configuration shown in (a). (c) Blurred configuration of the exciton confinement energy shown in (b). The configurations of the exciton confinement energy result in the sharp PL lines shown to the right of (b) and (c).

the PLE spectrum exhibits two distinct exciton peaks that arise from the absorption that creates the heavy-hole (HH) and light-hole (LH) excitons in the QW layer of the 3D-confined structure. When the excitation power was lowered to  $2 \mu\text{W}$ , the LH-exciton peak varied little, but the HH-exciton peak varied considerably. (The PLE spectrum at

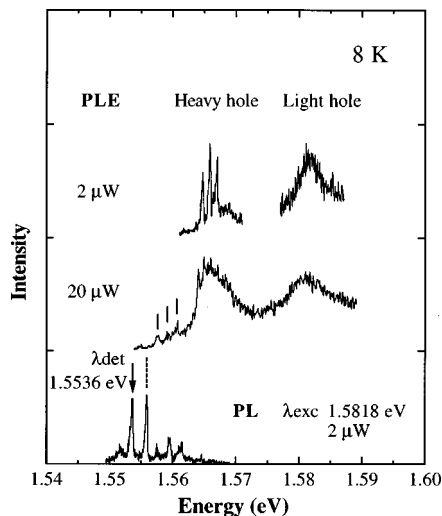


FIG. 4. PLE spectra of the single 3D-confined structure at  $P_{\text{exc}} = 20$  and  $2 \mu\text{W}$ . The bottom trace is its PL spectrum with well excitation at an energy and power of  $1.5818 \text{ eV}$  and  $2 \mu\text{W}$ , respectively. The PLE spectrum at  $P_{\text{exc}} = 2 \mu\text{W}$  was obtained only in parts of the energy range of the PLE spectrum at  $P_{\text{exc}} = 20 \mu\text{W}$ . The arrow in the bottom PL spectrum indicates the detection energy of the PLE spectra. The solid lines in the middle trace of the PLE spectrum indicate three weak lines located at lower energies than the intense HH-exciton transition.

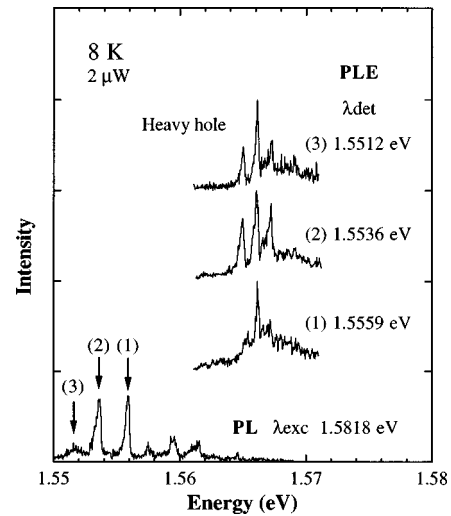


FIG. 5. HH-exciton transitions of the PLE spectra of the single 3D-confined structure at three detection energies. The detection energies were set at the PL lines indicated by the arrows in the bottom PL spectrum, which is the same as the bottom trace of Fig. 4.

$P_{\text{exc}} = 2 \mu\text{W}$  could only be obtained at exciton peaks.) As shown in the top-left trace in Fig. 4, the HH-exciton transition of the PLE spectrum changed to three sharp lines over a broad peak. The width of the sharp lines was about  $0.3 \text{ meV}$ , which is almost completely limited by the spectral resolution of our laser system. Note that an excitonic transition of the PLE spectrum split into multiple sharp lines. Such splitting has not been previously observed in the PLE spectra of QW heterostructures or 3D-confined structures.

Figure 5 shows HH-exciton peaks of the PLE spectra at  $P_{\text{exc}} = 2 \mu\text{W}$  for three detection energies. The detection energies were set at the PL lines indicated by the arrows in the bottom PL spectrum, which is the same as that in Fig. 4. Like the  $2\text{-}\mu\text{W}$  PLE spectrum in Fig. 4, each HH-exciton peak exhibited sharp lines over a broad peak. In contrast, the relative intensity of the sharp lines differed among the PLE spectra; that is, both sides of the sharp lines depended on the detection energies. However, the relative intensity also depended on the excitation power. In fact, the sharp lines obtained with a slightly higher excitation power had almost the same intensity for the PLE spectrum. The similar intensity suggests that a sharp line in the PLE spectrum is not directly related to any particular sharp line of the PL spectrum; in other words, the multiple PLE lines do not correspond to discrete excited states of a lateral potential well.

The above suggestion was supported by our measurements of the resonant PL spectra. Figure 6 shows the PL spectra at excitation energies resonant with the HH-exciton lines indicated by the arrows in the top PLE spectrum, and the PL spectrum at a nonresonant well-excitation energy for reference. All the resonant PL spectra showed almost the same features as the nonresonant PL spectrum. The similarity of the resonant behavior also suggests that a sharp line of the PLE spectrum is not directly related to any particular sharp line of the PL spectrum.

The sharp lines of the PLE spectra can be interpreted in terms of the HH-exciton absorption, whose energy is determined by the locally averaged thickness of the QW layer. It may be possible to assign each PLE line to absorption in QW



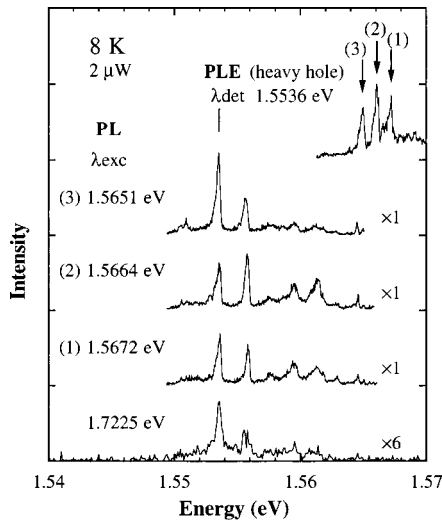


FIG. 6. (1)–(3) PL spectra of the single 3D-confined structure at excitation energies resonant with the HH-exciton lines (indicated by the arrows in the top PLE spectrum). The bottom trace shows the PL spectrum with non-resonant well excitation, whose energy was 1.7225 eV.

regions having different local thicknesses. However, the energy spacing of the sharp lines is about 1.3 meV, which is about half the calculated energy produced by monolayer fluctuation in the QW thickness. This “submonolayer” fluctuation can be explained in terms of interface microstructures. Heterointerfaces of QW’s are usually not atomically smooth even within an island. If one of the interfaces is atomically smooth and the other interface has a microstructure—that is, a small-scale structure with dimensions much smaller than the exciton diameter—the average thickness will differ by less than one monolayer from that of a QW layer where both the interfaces are atomically smooth. Thus, such interface microstructures would bring about a sub-monolayer difference in the locally averaged thickness. For example, the local thickness could have a submonolayer difference if the interfaces are smooth in parts and uniformly microrough in other parts.

Since the above discussion holds for LH-exciton transitions, LH-exciton peaks of PLE spectra should also split into sharp lines. However, as shown in the top-right trace of Fig. 4, the LH-exciton peak did not split. In the case of the HH-exciton peaks, the relative intensity of the sharp lines strongly depended on the excitation power. The excitation-power dependence suggests that the line splitting of the LH peaks might occur in the PLE spectra with a lower excitation power. In the present study, however, such measurements could not be done owing to insufficient sensitivity of our optical setup.

As shown in Fig. 4, the sharp lines of the PL spectrum occur at the lower energy side of the PLE peaks. Since the lines of the PL spectrum are due to the radiative recombination of HH excitons at the energy minima, the energy difference means that for the HH-exciton transition the recombination energy shifted by about 12 meV from the absorption energy to a lower energy. This energy shift is called a Stokes shift and is often seen in conventional QW heterostructures. The Stokes shift for QW heterostructures is explained by exciton localization to the potential islands of the QW

layer.<sup>25</sup> When we adopt the localization model, the Stokes shift obtained for the present sample corresponds to a fluctuation of about five monolayer in QW layer thickness. The magnitude of this Stokes shift is very large compared with that in conventional QW heterostructures where the magnitude is usually one or two monolayers. Thus, large interface fluctuations in layer thickness may exist even for single 3D-confined structures. This suggests that growth on patterned substrates specifically increases the depth of localized potentials. However, this increase does not seem to be a fatal phenomenon, because there is probably a difference in the preferred growth conditions for growth of QW heterostructures and growth of the pyramidal structure. Optimization of the conditions at the mesa-top region of pyramidal structures would reduce the interface fluctuations.

The PLE spectrum at  $P_{\text{exc}}$  of 20  $\mu\text{W}$  (Fig. 4) also exhibits three weak lines at the lower-energy side of the HH-exciton peak as indicated by the solid lines. Their spectral positions were equal to those of the three weak lines of the bottom PL spectrum. This correspondence of the spectral positions between the PL and PLE spectra suggests that the weak lines of the PL and PLE spectra are assigned to the same spatial origins of the potential islands where localized excitons recombine or are created. The weak-line intensity of the PL spectrum may imply that exciton transfer occurs from higher- to lower-energy states in the potential islands. In contrast to the three weak lines, there is no distinct line of the PLE spectrum corresponding to the intense line of the PL spectrum (as indicated in Fig. 4 by the broken line). From the viewpoint of exciton transfer, the lack of a distinct line may imply that at  $P_{\text{exc}}$  of 20  $\mu\text{W}$  the exciton transfer hardly occurs in the potential islands that are spatial origins of the intense PL lines. This suggests that the lateral distance between potential islands having a very deep-energy minima is great enough to prevent exciton transfer in the measured single structure.

To examine the uniformity of the optical property of single 3D-confined structures, we next measured the PL spectra of three structures separated with an interval of about 9  $\mu\text{m}$  at  $P_{\text{exc}}$  of 250 nW. As shown in Fig. 7, each resultant spectrum exhibited sharp lines, but they vary in number, width, intensity, and energy position among the PL spectra. The optical properties thus varied widely, even in neighboring single structures. This wide variation indicates a large diversity in the interface fluctuations among the single 3D-confined structures.

We also measured the single structure [numbered (3) in Fig. 7] at a lower excitation power ( $P_{\text{exc}}=25$  nW) and higher spectral resolution. The resultant spectrum shown in the inset of Fig. 7 reveals that the sharp PL line split into extremely sharp lines whose width of 0.04 meV was almost completely limited by the spectral resolution of our optical setup. The energy spacing of these extremely sharp lines was about 0.1 meV.

Next, we will consider the origin of the fine splitting of the sharp lines. Extremely sharp luminescent lines from 3D-confined structures are generally believed to be evidence of a discrete density of states in quantum dots. Several groups have reported observing a series of extremely sharp PL lines through microphotoluminescence measurement of thin QW’s formed with growth interruptions at interfaces.<sup>26–30</sup> These

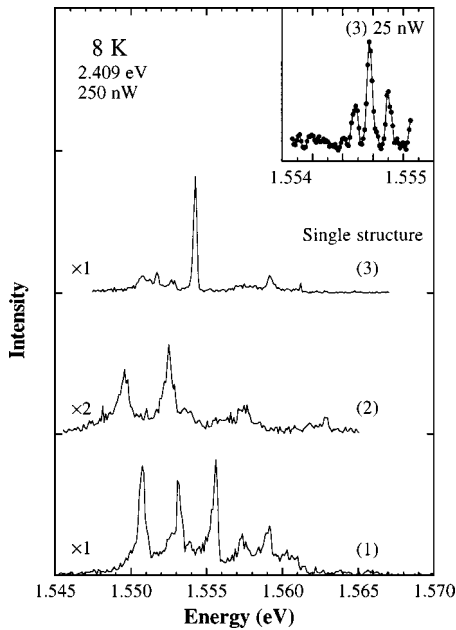


FIG. 7. PL spectra of three single 3D-confined structures at  $P_{\text{exc}}$  of 250 nW. The excitation energy was 2.409 eV, corresponding to the barrier excitation. The inset shows the PL spectrum of the third single structure (3) with lower excitation power ( $P_{\text{exc}} = 25$  nW) and higher spectral resolution.

extremely sharp lines, which were less than 0.1 meV wide, were attributed to the radiative recombination of excitons in the ground and excited states of quantum dots defined by the potential from the interface fluctuations.<sup>27–30</sup>

However, the spectral sharpness mainly arises from the excitonic effect, which does not depend directly on the shape of the density of states. In fact, Andreani, Tassone, and Bassani calculated the homogeneous linewidth of excitons in QW heterostructures and obtained a value of 0.026 meV for excitons in GaAs/ $\text{Al}_x\text{Ga}_{1-x}\text{As}$  QW's of about 10 nm.<sup>31</sup> Since the linewidth of the PL spectrum in the inset is close to this value, it is likely to be related to the homogeneous broadening in the QW heterostructure of the 3D-confined structure. Actually, the luminescent lines of an exciton localized in a small potential island have a homogeneous linewidth because all inhomogeneous broadening is removed. From our estimation of the time-averaged number of electron-hole pairs, we found that 0.15 of a pair is confined in the single structure for barrier excitation at  $P_{\text{exc}}$  of 25 nW. We therefore believe that the extremely sharp linewidth is almost completely determined by the homogeneous linewidth that arises from the radiative recombination of a single exciton localized in an individual potential island.<sup>32</sup>

If localized potential islands are sufficiently small, each extremely sharp line in the inset would be due to the radiative recombination of a 3D-quantized exciton. However, the splitting from the sharp line ( $\cong 0.5$  meV) to the extremely sharp lines ( $\cong 0.04$  meV) was not due to the three-dimensional quantization. That is, the extremely sharp lines did not indicate excited states of a 3D-quantized exciton in a potential island, because the energy spacing of the extremely sharp lines ( $\cong 0.1$  meV) was much smaller than that expected for excited states in a quantum dot ( $>1$  meV).

We propose a different explanation for the line splitting.

The above discussion suggests that each of the extremely sharp lines corresponds to the recombination of single excitons localized into different potential islands. Hence, a possible origin of the line splitting is a difference in the confinement energy of localized excitons. The luminescent energy is almost completely determined by the local thickness of the QW layer at the recombination centers of the potential islands. However, as mentioned in our discussion of the sharp PLE lines, heterointerfaces are usually not atomically smooth within an island. A small change in the microstructures of interface islands will cause small shifts in the exciton confinement energy.<sup>33,34</sup> As a result, the steplike feature of the confinement-energy configuration blurs owing to the position dependence of microstructures in a QW layer. [see, for example, Fig. 3(b) and (c)]. This means that the recombination energy changes by a small amount within spatially isolated islands that have almost the same local thickness but differ in size and microstructure. Thus, the line splitting in the inset of Fig. 7 may indicate the existence of microstructures in the QW heterostructure of the 3D-confined structure. We believe that all the sharp lines of the PL spectra at  $P_{\text{exc}} = 250$  nW shown in Fig. 7 are also a superposition of several extremely sharp lines whose spectral positions are slightly different.

Finally, we comment on the previous CL measurements of 3D-confined structures fabricated by growth on patterned substrates.<sup>10,13</sup> Although the sizes of the measured structures were within the regime of three-dimensional quantum confinement, their CL spectra exhibited broad peaks that were about 10 meV wide and, consequently, did not exhibit sharp lines. Our present data concerning the excitation-power dependence suggests that a principal cause of the broadening is intense electron-beam excitation. CL measurements with much weaker excitation would exhibit sharp CL lines from the structures. We also note the significance of observing sharp luminescent lines from the disklike 3D-confined structure which was not within the quantum-confinement regime. This observation indicates that sharp luminescent lines do not necessarily provide evidence of successful fabrication of quantum dots.

#### IV. CONCLUSIONS

We have measured the PL and PLE spectra of single 3D-confined GaAs/AlAs structures having a 10-nm vertical thickness and a 0.2- $\mu\text{m}$  lateral width. Consistent with previous reports on CL measurements of 3D-confined structures within the regime of three-dimensional quantum confinement,<sup>11,16</sup> the PL and PLE spectra of a spatially isolated single structure exhibited broad exciton peaks several meV wide at high-excitation power. However, when the excitation power was lowered, each heavy-hole exciton peak in the PL and PLE spectra became a series of sharp lines whose widths were respectively about 0.5 and 0.3 meV. The sharp PL lines were probably due to the recombination of excitons localized into lateral potential islands in the single structure. In the PL spectrum at a lower excitation power, a sharp line split into extremely sharp lines, whose width of 0.04 meV was almost completely limited by the spectral resolution of our optical setup. We proposed a possible origin of this fine splitting: The splitting may represent differ-

ences in the confinement energy of excitons localized in potential islands that have almost the same local thickness but differ in size and microstructure. From our analysis of the PLE spectra and the resonant PL spectra, we conclude that a sharp line in a PLE spectrum is not directly related to any particular sharp line of a PL spectrum. The PLE sharp lines can be interpreted in terms of the exciton absorption, whose energy is determined by the locally averaged thickness of the 3D-confined structure. The observation of sharp luminescent lines from a disklike 3D-confined structure that is not within the quantum-confinement regime indicates that sharp luminescent lines do not necessarily provide evidence of the successful fabrication of quantum dots.

By performing epitaxial growth on the patterned substrate, we fabricated 3D-confined structures on a sub- $\mu\text{m}$

scale and obtained sharp luminescent lines from them. This high-optical quality indicates that epitaxial growth on patterned substrates is a promising technique for fabricating quantum dots. Fabricating 3D-confined structures with sizes within the quantum-confinement regime by this growth method, which is superior for controlling the structure's density and position, provides an attractive opportunity for detailed optical measurements of a single-quantum dot and is a possible source of novel devices.

#### ACKNOWLEDGMENT

We thank Dr. M. López for his valuable discussions concerning growth on patterned substrates.

\*Present address: Tsukuba Advanced Research Alliance Center, University of Tsukuba, 1-1-1 Tennou, Tsukuba, Ibaraki 300-8577, Japan.

<sup>1</sup>*Nanostructures and Quantum Effects*, edited by H. Sakaki and H. Noge (Springer, Berlin, 1994).

<sup>2</sup>*Proceedings of the Seventh International Conference on Modulated Semiconductor Structures, Madrid, Spain, 1995*, edited by C. Tejedor and L. Viña [*Solid-State Electron.* **40** (1996)].

<sup>3</sup>*Proceedings of the 23rd International Conference on the Physics of Semiconductors, Berlin, Germany, 1996*, edited by M. Scheffler and R. Zimmermann (World Scientific, Singapore, 1997).

<sup>4</sup>L. Goldstein, F. Glas, J. Y. Marzin, M. N. Charasse, and G. LeRoux, *Appl. Phys. Lett.* **47**, 1099 (1985).

<sup>5</sup>D. Lenard, M. Krishnamurthy, C. M. Reaves, S. P. Denbaars, and P. M. Petroff, *Appl. Phys. Lett.* **63**, 3203 (1993).

<sup>6</sup>J.-Y. Marzin, J.-M. Gérard, A. Izraël, D. Barrier, and G. Bastard, *Phys. Rev. Lett.* **73**, 716 (1994).

<sup>7</sup>M. Grundmann, J. Christen, N. N. Ledentsov, J. Böhrer, D. Bimberg, S. S. Ruvimov, P. Werner, U. Richter, U. Gösele, J. Heydenreich, V. M. Ustinov, A. Y. Egorov, A. E. Zhukov, P. S. Kop'ev, and Z. I. Alferov, *Phys. Rev. Lett.* **74**, 4043 (1995).

<sup>8</sup>R. Leon, P. M. Petroff, D. Leonard, and F. Farad, *Science* **267**, 1966 (1995).

<sup>9</sup>For example, E. Kapon, in *Semiconductors and Semimetals*, edited by A. C. Gossard (Academic, New York, 1994), Vol. 40, p. 259.

<sup>10</sup>A. Madhukar, K. C. Rajkumar, and P. Chen, *Appl. Phys. Lett.* **62**, 1547 (1993).

<sup>11</sup>K. C. Rajkumar, A. Madhukar, K. Rammohan, D. H. Rich, P. Chen, and L. Chen, *Appl. Phys. Lett.* **63**, 2905 (1993).

<sup>12</sup>M. López, T. Ishikawa, and Y. Nomura, *Electron. Lett.* **29**, 2225 (1993).

<sup>13</sup>K. C. Rajkumar, A. Madhukar, P. Chen, A. Konkar, L. Chen, K. Rammohan, and D. H. Rich, *J. Vac. Sci. Technol. B* **12**, 1071 (1994).

<sup>14</sup>A. Konkar, K. C. Rajkumar, Q. Xie, P. Chen, A. Madhukar, H. T. Lin, and D. H. Rich, *J. Cryst. Growth* **150**, 311 (1995).

<sup>15</sup>M. López, N. Tanaka, I. Matsuyama, and T. Ishikawa, *Appl. Phys. Lett.* **68**, 658 (1996).

<sup>16</sup>D. H. Rich, H. T. Lin, A. Konkar, P. Chen, and A. Madhukar, *Appl. Phys. Lett.* **69**, 665 (1996).

<sup>17</sup>J. Kasai, S. Tanaka, K. Higuchi, and Y. Katayama, *J. Vac. Sci. Technol. B* **15**, 862 (1997).

<sup>18</sup>*Confocal Microscopy*, edited by T. Wilson (Academic, London, 1990).

<sup>19</sup>J. Kasai and Y. Katayama, *Rev. Sci. Instrum.* **66**, 3738 (1995); **67**, 4397 (1996).

<sup>20</sup>U. Bockelmann, W. Heller, A. Filoramo, and Ph. Roussignol, *Phys. Rev. B* **55**, 4456 (1997).

<sup>21</sup>This is the mean value of the carrier lifetime reported by H. Watabe, Y. Nagamune, F. Sogawa, and Y. Arakawa, *Solid-State Electron.* **40**, 537 (1996). They described the excitation-power dependence of carrier lifetime in a 3D-confined GaAs/Al<sub>x</sub>Ga<sub>1-x</sub>As structure whose nominal size was similar to that of our sample. The lifetime in the well-excitation case decreased from 400 to 200 ps as the averaged excitation power decreased from 100 to 1  $\mu\text{W}$ . From an estimation similar to that in Ref. 20, we found that the pair number excited by one pulse of the laser used with their 3D-confined structure amounts to 250 for an excitation power of 10  $\mu\text{W}$ .

<sup>22</sup>See, for example, R. Cingolani and K. Ploog, *Adv. Phys.* **40**, 535 (1991).

<sup>23</sup>There are many reports of multiple luminescent lines caused by monolayer steps in the layer thickness of QW's, which were formed with growth interruptions at the interfaces. [See, for example, H. Sakaki, M. Tanaka, and J. Yoshino, *Jpn. J. Appl. Phys.*, Part 2 **24**, L417 (1985); T. Fukunaga, K. L. I. Kobayashi, and H. Nakashima, *ibid.* **24**, L510 (1985).] However, there was no growth interruption at the GaAs/AlAs interfaces for our sample.

<sup>24</sup>The PL spectrum exhibits a different feature, compared with the PL spectrum shown in the bottom trace of Fig. 2, although the same single structure was measured. This indicates the dependence of the PL spectra on excitation energy. The PL spectra from the well excitation at various energies revealed almost the same traces. This suggests that the variation in the spectral feature is due to a difference in the excitation conditions, i.e., the well excitation or barrier excitation. However, we do not have sufficient data to discuss this in detail, and further study is required to clarify the dependence of the PL spectra on the excitation condition.

<sup>25</sup>G. Bastard, C. Delalande, M. H. Meynadier, P. M. Frijlink, and M. Voos, *Phys. Rev. B* **29**, 7042 (1984).

<sup>26</sup>H. F. Hess, E. Betzig, T. D. Harris, L. N. Pfeiffer, and K. W. West, *Science* **264**, 1740 (1994).

<sup>27</sup>K. Brunner, G. Abstreiter, G. Böhm, G. Tränkle, and G. We-

- imann, Appl. Phys. Lett. **64**, 3320 (1994); Phys. Rev. Lett. **73**, 1138 (1994).
- <sup>28</sup>D. Gammon, E. S. Snow, and D. S. Katzer, Appl. Phys. Lett. **67**, 2391 (1995).
- <sup>29</sup>D. Gammon, E. S. Snow, B. V. Shanabrook, D. S. Katzer, and D. Park, Phys. Rev. Lett. **76**, 3005 (1996); Science **273**, 87 (1996).
- <sup>30</sup>D. Hessmann, P. Castrillo, M.-E. Pistol, C. Pryor, and L. Samuelson, Appl. Phys. Lett. **69**, 749 (1996).
- <sup>31</sup>L. C. Andreani, F. Tassone, and F. Bassani, Solid State Commun. **77**, 641 (1991).
- <sup>32</sup>A homogeneously broadened line is Lorentzian in line shape. [See for example, R. Loudon, *The Quantum Theory of Light* (Oxford University Press, Oxford, 1983).] In our study, however, the line shape in the inset of Fig. 7 was almost completely limited by the spectral resolution of our optical setup. The line shape can be approximated by a triangle which is the spectral resolution shape. Thus, we were unable to discuss the homogeneous broadening in terms of the line shape.
- <sup>33</sup>C. A. Warwick, W. Y. Jan, A. Ourmazd, and T. D. Harris, Appl. Phys. Lett. **56**, 2666 (1990).
- <sup>34</sup>D. Gammon, B. V. Shanabrook, and D. S. Katzer, Phys. Rev. Lett. **67**, 1547 (1991).